

Turn-Off Loss Improvement by IGBT Scaling

Munetoshi Fukui¹, Takuya Saraya¹, Kazuo Itou¹, Toshihiko Takakura¹, Shinichi Suzuki¹, Kiyoshi Takeuchi¹, Kuniyuki Kakushima², Takuya Hoshii², Kazuo Tsutsui², Hiroshi Iwai², Shin-ichi Nishizawa³, Ichiro Omura⁴ and Toshiro Hiramoto¹

¹Institute of Industrial Science, The University of Tokyo, Tokyo, Japan,

Phone: +81-3-5452-6264 E-mail: fukui@nano.iis.u-tokyo.ac.jp

²Tokyo Institute of Technology, Yokohama, Japan, ³Kyushu University, Kasuga, Japan

⁴Kyushu Institute of Technology, Kitakyushu, Japan

Abstract

Effects of IGBT scaling on turn-off characteristics were studied by TCAD simulations. It was found that the scaling can reduce turn-off loss without degrading on-state loss ($V_{ce,sat}$), owing to stronger IE effect (i.e. higher top side carrier concentration) and improved resistance to dynamic avalanche.

1. Introduction

Power semiconductor devices are key components of the modern industry. Among them, Insulated Gate Bipolar Transistors (IGBTs) [1,2] are widely used for high power applications. Recently, an IGBT scaling concept [3] has been proposed. It is reported that, by scaling down the dimensions of the trench-gated emitter both vertically and horizontally, on-state voltage ($V_{ce,sat}$) can be reduced [3,5], owing to the injection enhancement (IE) effect [4]. In addition, it was experimentally demonstrated that the IGBT scaling also decreases turn-off loss [6,7], though the reason for this was not fully understood. Therefore, in this work, TCAD simulations were performed to clarify the effects of IGBT scaling on turn-off loss.

2. Analysis Method

Reference ($k=1$) and scaled ($k=3$) 3.3 kV class IGBTs (Fig.1) were simulated. The topside MOS structure dimensions were scaled by 1/3, though the trench width was kept constant to align with experiments [7]. The gate oxide thicknesses for $k=1$ and $k=3$ were 100 nm and 33 nm, respectively. Carrier lifetime was assumed to be independent from k . At the backside, a field stop structure was adopted, and the P-collector boron concentration was varied. Turn-off characteristics were analyzed in an inductive load circuit with 1700 V operation voltage (V_{cc}) and 80 A current (I_o). Parasitic components were ignored. Gate voltage source swings of $k=1$ and $k=3$ IGBTs were ± 15 V and ± 5 V, respectively.

3. Analysis Results

Fig.2 shows typical on-state I - V characteristics as well as $V_{ce,sat}$ dependence on P-collector doping. $V_{ce,sat}$, which determines the on-state power loss, is improved by the scaling thanks to the enhanced IE effect.

Fig.3 (a) shows typical turn-off waveforms for different collector voltage rising rates (dV/dt), which can be increased by reducing the gate series resistance. Turn-off loss E_{off} is given as the sum of E_{vr} and E_{cf} (Fig.3 (b)). Higher dV/dt is beneficial for reducing E_{vr} . However, Fig.3 shows that, while normal operation is realized when $dV/dt=1$ kV/ μ s, too large $dV/dt=2$ kV/ μ s causes an early V_{ge} drop and inflection of the V_{ce} vs time waveform. These are the indication of

dynamic avalanche (DA); Due to the limited carrier velocity, too fast voltage swing results in insufficient depletion layer expansion and impact ionization. Fig.4 shows that holes are generated near the trench bottom when the avalanche starts. DA must be avoided for reliable operations, and will set a limit on the turn-off speed.

E_{vr} and E_{cf} were calculated by systematically varying dV/dt and P-collector doping for both $k=1$ and 3 (Figs.5 and 6). Fig.5 shows that E_{vr} does not depend on k , and is simply inversely proportional to dV/dt , as long as DA is not present. However, there is a major difference that the onset dV/dt of DA for $k=3$ is much larger than that for $k=1$. It is speculated that the reduced mesa width relieved the field confinement near the trench bottom. Fig.6 shows that E_{cf} , that is governed by the amount of stored carrier near the P-collector, increases approximately in proportion to P-collector doping and dV/dt . It is considered that large dV/dt will hinder transport of back side carrier to the front side, resulting in increased stored carrier concentration.

Fig.7 shows $E_{off}=E_{vr}+E_{cf}$ vs $V_{ce,sat}$ relationships converted from the data in Figs.2, 5 and 6. When $dV/dt=1$ kV/ μ s, though $E_{vr}\sim 100$ mJ dominates, $k=3$ devices show lower E_{off} due to reduced E_{cf} . This is because, a $k=3$ device can achieve equal $V_{ce,sat}$ as $k=1$ by lower P-collector doping due to the enhanced IE effect, which results in lower amount of back side stored carrier (Fig.8). The difference between $k=1$ and 3 becomes more pronounced when $dV/dt=2$ kV/ μ s, since E_{cf} is reduced. In addition, a $k=3$ device can achieve much lower $V_{ce,sat}$ than $k=1$ without suffering from DA.

4. Conclusions

Effects of IGBT scaling on turn-off loss were systematically studied using TCAD simulations. It was shown that the scaling is beneficial, not only for improving on-state loss, but also for reducing turn-off loss, owing to stronger IE effect and larger tolerance to dynamic avalanche.

Acknowledgements

Authors are deeply grateful to Dr. K. Satoh in Mitsubishi Electric Corp., Dr. T. Matsudai in Toshiba Electronic Devices & Storage Corp. and Dr. M. Tsukuda in Green Electronics Research Institute for earnest discussions. This work is based on results obtained from a project commissioned by the New Energy and Industrial Technology Development Organization (NEDO).

References

- [1] N. Iwamuro *et al.*, IEEE Trans. ED, 64, p.741, 2017.
- [2] H. Feng *et al.*, ISPSD, p.203, 2016.
- [3] M. Tanaka *et al.*, Solid-State Electronics, 80, p.118, 2013.
- [4] M. Kitagawa *et al.*, IEDM, p.679, 1993.
- [5] K. Kakushima *et al.*, IEDM, p.268, 2016.
- [6] T. Saraya *et al.*, IEDM, p.189, 2018.
- [7] T. Saraya *et al.*, ISPSD, to be presented, 2019.

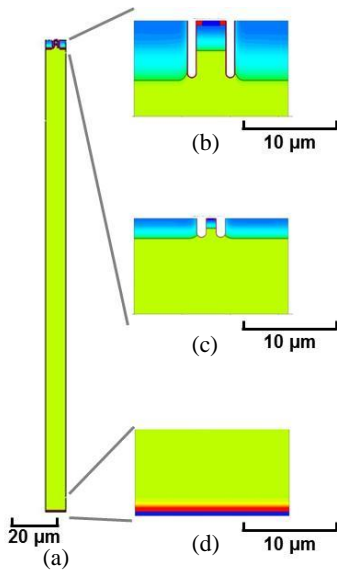


Fig.1 Simulated IGBT structure: (a) whole view, (b) $k=1$ top side, (c) $k=3$ top side, (d) bottom side.

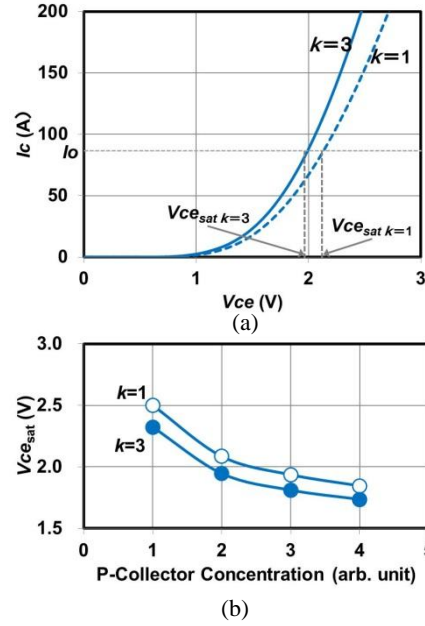


Fig.2 On-state characteristics: (a) typical $I-V$, and (b) $V_{ce,sat}$ vs. P-collector concentration.

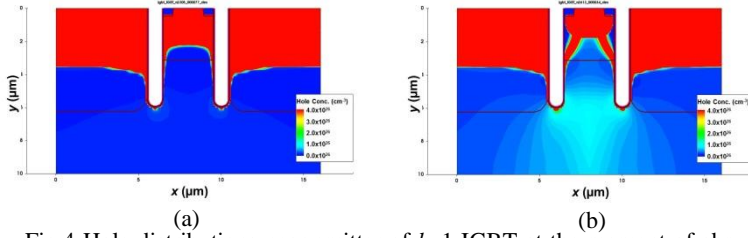


Fig.4 Hole distributions near emitter of $k=1$ IGBT at the moment of abrupt gate voltage drop, for (a) $dV/dt=1$ kV/ μ s, and (b) $dV/dt=2$ kV/ μ s.

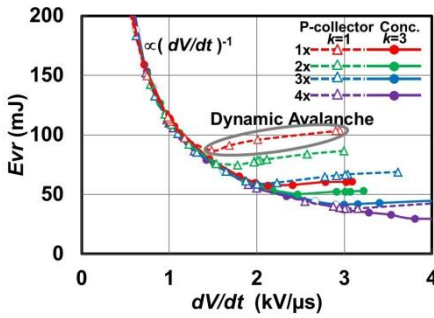


Fig.5 Dependence of E_{vr} on dV/dt .

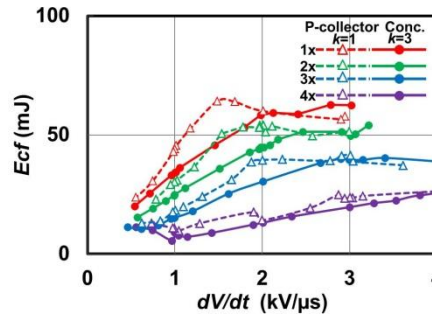


Fig.6 Dependence of E_{cf} on dV/dt .

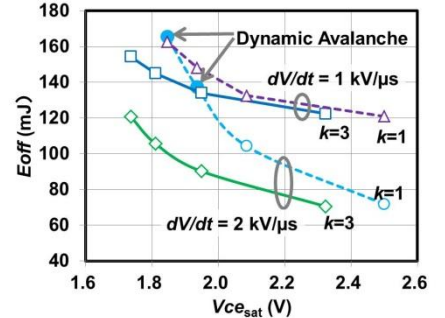


Fig.7 Trade off between E_{off} and $V_{ce,sat}$.

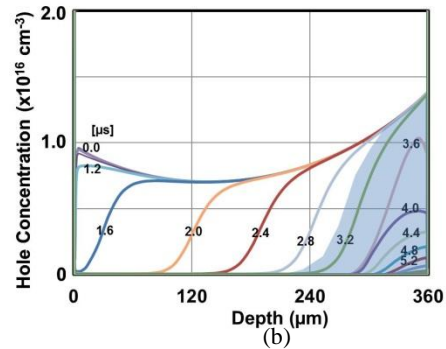
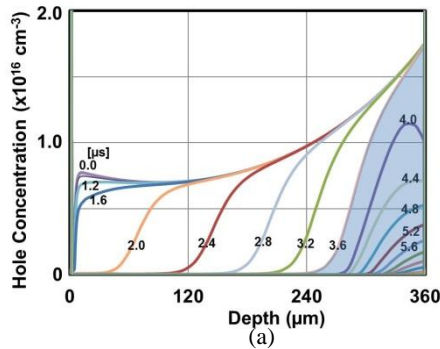


Fig.8 Hole distributions during turn-off process for (a) $k=1$ and (b) $k=3$. $dV/dt=1$ kV/ μ s, $V_{ce,sat}=1.95$ V, normal operation cases without DA for both devices. Hatched areas show stored carrier distributions at gate voltage drop.

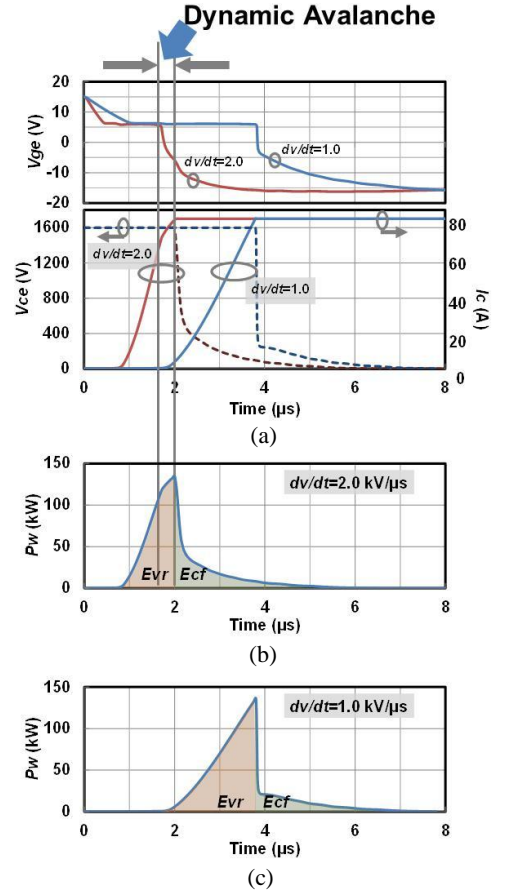


Fig.3 Typical turn-off waveforms of $k=1$ IGBT: (a) V_{ge} , V_{ce} and I_c , vs. time, and power dissipation vs. time for (b) $dV/dt=2.0$ kV/ μ s, and (c) $dV/dt=1.0$ kV/ μ s.